Journal of Bio- and Tribo-Corrosion (2020) 6:104
https://doi.org/10.1007/s40735-020-00394-3

Adenium obesum Extract as a Safe Corrosion Inhibitor for C-Steel in NaCl Solutions: Investigation of Biological Effects

Abd El-Aziz S. Fouda[1] · **Mohamed Eissa**[2,3]

Received: 18 October 2019 / Revised: 20 June 2020 / Accepted: 13 July 2020 / Published online: 29 July 2020

Abstract
In this paper, the impacts of polluted NaCl (3.5% NaCl + 16 ppm Na_2S) on the corrosion of C-steel (CS) at different temperatures and in presence of different concentrations of *Adenium obesum* extract (AOE) were considered by chemical, electrochemical techniques and other surface examination tests. The outcomes demonstrate that the corrosion rate of CS diminishes with increment of inhibitor doses. % IE reached to ≈90% at 300 ppm AOE.The acquired outcomes showed that the examined extract is physically adsorbed on the CS surface and followed Temkin adsorption isotherm. The potentiodynamic polarization (PP) information revealed that this extract goes about as mixed kind inhibitor. The results got from the various techniques are in great agreement.

Keywords *Adenium obesum* extract (AOE) · Carbon steel · Polluted NaCl · biological effect

1 Introduction

Consumption of materials causes enormous misfortunes in the economy of numerous nations because of the colossal measure of assets expected to lessen it. The corrosion inhibition of metals, particularly of CS, has gotten some consideration as a result of its astounding mechanical properties, minimal effort and far reaching use in the business, for example, substance handling, oil generation, refining, transportation, pipelines, mining, development industry, marine applications, hence, looks into in the field of consumption restraint of steel is important. Seawater contains the remaining parts of dead life forms, coral reefs, ships, and pontoons which all are decay and prompt acceleration of gases, for example, H_2S and Na_2S and different gases respond with chlorine and hydrogen deliver contaminated NaCl. Among the few strategies for consumption, control is the utilization of inhibitors. The investigations of plant extracts as consumption inhibitors are of awesome enthusiasm from an ecological point of view and are drawing in a huge level of consideration [1–3]. The well-being and ecological issues of corrosion inhibitors emerged in businesses has dependably been a worldwide concern. Plant extract is minimal effort and natural safe, so the primary favorable circumstances of utilizing plant removes as corrosion inhibitors are financial and safe condition. A few examinations have been completed on the security of corrosion of metals and compounds by plant extracts [4–15]. Nonetheless, there is as yet a requirement for look into on different plants can be utilized as inhibitors in mechanical applications. This present investigation looks to discuss the AOE as green inhibitor for protecting CS from corrosion in polluted NaCl.

2 Material and Solutions

2.1 Materials

Tests were undergone on rectangular examples with dimensions 2×2×0.1 cm of CS with the following chemical composition in wt%: C 0.200, Mn 0.350, P 0.024, Si 0.003, and Fe balance. CS samples (2×2×0.2 cm) automatically skinned with totally different grades (22–1200) of sandpaper and polished by 0.25 µm aluminum oxide powder to approach the mirror surface, then degreased, hand washed with bidistilled water and rinsed with ethanol, and finally used in weight loss tests.

✉ Abd El-Aziz S. Fouda
asfouda@hotmail.com

[1] Chemistry Department, Faculty of Science, Mansoura University, Mansoura 35516, Egypt

[2] College of Science & Humanities-Harimlae, Shaqra University, Shaqraa, Saudi Arabia

[3] Present Address: Higher Institute of Engineering & Technology, KMA, Alex, Egypt

2.2 Solution Preparation

The polluted sodium chloride (3.5% NaCl + 16 ppm Na_2S) solution was prepared from NaCl and Na_2S and bidistilled water. The concentration range of AOE varied from 50 to 300 ppm and the electrolyte used was 100 ml for each experiment.

2.3 Plant Extraction

The powered stembark of *Adenium obesum* (500 g) was packed into a thimble and placed inside a Soxhlet extractor and extracted exhaustively and, respectively, with petroleum spirit (60–80 °C) and methanol (1 l each). The extracts were concentrated in vacuum at 40 °C using rotary evaporator, after which the crude extracts were obtained from the solvents [16]. 1 g of this crude extract was dissolved in little amount of dimethyl formamide (DMF) and completed to 1 l by ethanol to prepare stock solution (1000 ppm). The concentrations were obtained by dilution by bidistilled water.

2.4 Phytochemical Screening

The petroleum and methanolic extracts of the stembark of *A. obesum* were subjected to preliminary phytochemical tests to detect the presence of alkaloids, steroids, saponins, glycosides, anthraquinones, tannins, terpenoids, coumarins, carbohydrates, and flavonoids [17] using standard techniques.

Phytochemical constituents of *Adenium obesum* (stembark) extract.

S/No.	Phytochemicals	Results
		methanolic extract
1	Carbohydrates	+
2	Steroids	+
3	Terpenoids	+
4	Saponins	+
5	Tannins	+
6	Anthraquinones	+
7	Cardiac glycosides	+
8	Alkaloids	+
9	Coumarins	-
10	Flavonoids	+

key:+/- = presence, absence of phytochemical tested

2.5 Methods

2.5.1 Weight Loss (WL) Technique

The coins were dipping in 100 ml of polluted NaCl and existence of the various contents of AOE is set in water thermostat. After 3 h, the samples were removed, rinsed, dried, and weighed again. The % IE and the θ were founded from Eq. (1)

$$\%\ \mathrm{IE} = \theta \times 100 = \left[\left(W_o - W\right)/W_o\right] \times 100, \tag{1}$$

where W_o and W are the weights of nonexistence and occurrence of AOE, individually.

2.5.2 Open-Circuit Potential (EOC) Method

The working electrode was immersed in polluted NaCl (100 ml) for 20 min to establish a steady-state EOCP.

2.5.3 Potentiodynamic Polarization Technique

This technique was done in a typical three compartment glass cell. The potential range was (− 1.0 to − 0.6 V vs. SCE) at OCP with a scan rate 1 mV s^{-1}.

2.5.4 EIS Technique

This technique was done by AC signs of 5 mV peak-to-peak amplitude and at frequency range of 10^7 Hz to 0.1 Hz. The (% IE) and θ were found from Eq. (2) [18]:

$$\%\ \mathrm{IE} = 100 \times \theta = 100 \times \left[\left(R_{ct} - R_{ct}^{o}\right)/R_{ct}\right], \tag{2}$$

where R_{ct}^{o} and R_{ct} are the charge transfer resistances without and with AOE, individually.

2.5.5 EFM Test

This technique used two frequencies of range 2 and 5 Hz depended on three conditions [19]. The i_{corr}, $\beta_{c,}$ and β_a and CF-2, CF-3 (causality factors) were measured by the greater two peaks [20].

2.5.6 Surface Examination

Al alloy pieces were dipped in testing solutions for 1 day. Then, they were polished, dried, and analyzed by SEM, FT-IR, and AFM.

3 Results and Discussion

3.1 Weight Loss (WL) Tests

WL–time curves of CS in polluted NaCl have been determined in existence and nonexistence of various AOE doses, which have been shown in Fig. 1. The gained corrosion parameters data have been reported in Table 1, from which we have been finding that % IE raises with rising AOE doses and raises with rising temperature. Lowering in corrosion rate (CR) by rising AOE doses is as a result of the fact that the metal surface coverage (θ) becomes larger via the adsorption of inhibitor molecules [21]. The reduction in CR possibly with rising in temperature via adsorption rate of AOE on the CS surface has been raised at higher temperatures [22].

3.2 Adsorption Isotherms

AOE is adsorbed on the CS surface due to that the interaction energy among the CS surface and the extract is more than that between H_2O molecules and metal [23, 24]. From the data, the Temkin model adsorption isotherms fit in the excellent manner (Fig. 2). The Temkin adsorption isotherm may be expressed by:

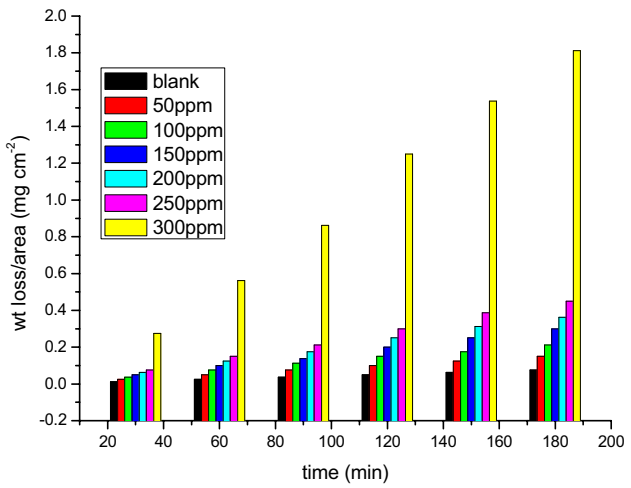

Fig. 1 Corrosion of C-steel in polluted NaCl in the absence and presence of different concentrations of AOE at 30 °C

$$a\theta = \ln K_{ads} C, \tag{3}$$

where C is concentration of the extract.

3.3 Thermodynamic Parameters

The thermodynamic activation energy (E_a^*) was calculated [25] from the corrosion rate data obtained from weight loss experiments using the Eq. 4 and are listed in the Table 2. E_a^* was estimated from Arrhenius equation:

Table 1 Variation of surface coverage (θ), degree of efficiency (% IE), and corrosion rate (k_{corr}) of AOE at 120 min immersion in polluted NaCl at different temperatures

Temperature (°C)	[inh] (ppm)	k_{corr} (mg cm^{-2} min^{-1}) × 10^3	θ	% IE
30	Blank	10.4	–	–
	50	2.50	0.877	87.7
	100	2.08	0.897	89.7
	150	1.66	0.918	91.8
	200	1.25	0.938	93.8
	250	0.833	0.959	95.9
	300	0.417	0.970	97.0
35	Blank	11.5	–	–
	50	3.33	0.855	85.5
	100	2.91	0.873	87.3
	150	2.51	0.890	89.0
	200	2.10	0.909	90.9
	250	1.70	0.927	92.7
	300	1.26	0.950	95.0
40	Blank	13.0	–	–
	50	4.16	0.840	84.0
	100	3.75	0.857	85.7
	150	3.33	0.872	87.2
	200	2.93	0.888	88.8
	250	2.55	0.904	90.4
	300	2.11	0.928	92.8
45	Blank	14.7	–	–
	50	5.00	0.818	81.8
	100	4.58	0.833	83.3
	150	4.11	0.848	84.8
	200	3.80	0.863	86.3
	250	3.40	0.879	87.9
	300	2.48	0.910	91.0
50	Blank	18.6	–	–
	50	5.83	0.792	79.2
	100	5.41	0.807	80.7
	150	5.03	0.822	82.2
	200	4.60	0.837	83.7
	250	4.13	0.851	85.1
	300	3.81	0.867	86.7

$$\Delta G^{o}_{ads} = \Delta H^{o}_{ads} - T\Delta S^{o}_{ads}, \quad (4)$$

$$K_{ads} = (1/55.5)\exp\left(-\Delta G^{o}_{ads}/RT\right), \quad (5)$$

$$k_{corr} = A\exp\left(-E^{*}_{a}/RT\right), \quad (6)$$

where "A = Arrhenius constant, R = gas constant and k = rate of corrosion." Figure 3 is plotted between log k_{corr} vs. 1/T for various concentration of *A. obesum* extract. From the figure, the E^{*}_{a} value can be calculated from the slope of the line. The ΔH^{*} and the ΔS^{*} can be computed using another formula of transition state expression [26–28]

$$k_{corr} = (RT/Nh)\exp(\Delta S^{*}/R)\exp(\Delta H^{*}/RT), \quad (7)$$

where "h = Planck's constant and N = Avogadro's number." The data of ΔH^{*} and ΔS^{*} can be measured by plotting log (k_{corr}/T) vs. 1/T (Fig. 4). The data of E^{*}_{a}, ΔS^{*} and ΔH^{*} are shown in Table 3.

3.4 Potentiodynamic Polarization Measurements

The potentiodynamic polarization curves for CS in the numerous concentrations of AOE at 25 °C are shown in Fig. 5. From the figure, one can noted that both (discharge hydrogen) cathodic and (CS dissolution) anodic reactions were inhibited by adding various concentration of AOE. Both β_a and β_c were raped to positive and negative directions, respectively. The chemical science parameters, E_{corr}, β_a and β_c, θ, % IE and i_{corr} were measured and given in Table 4. Data shows that by addition of extract the values of i_{corr} were lowered whereas the values of E_{corr} and β_a and β_c had no vital modification. So, the AOE performance as mixed type inhibitor.

3.5 EFM Tests

The data obtained from EFM for CS in 0.5 M H_2SO_4 at various concentration of AOE at 25 °C were measured and

Table 2 Adsorption parameters for AOE in polluted NaCl obtained from Temkin adsorption isotherm at different temperatures

Temperature (°C)	K_{ads} (M^{-1})	$\Delta G_{ads}{}^{o}$ (kJ mol^{-1})
30	14.15	33.6
35	23.93	34.9
40	25.36	35.1
45	35.477	35.9
50	281.2	41.0

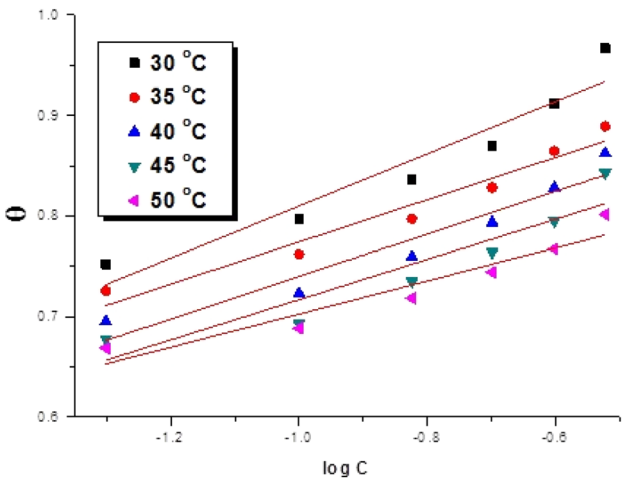

Fig. 2 Temkin adsorption isotherm plotted as θ vs. log C of AOE for corrosion of C-steel in polluted NaCl solution from weight loss method at different temperatures

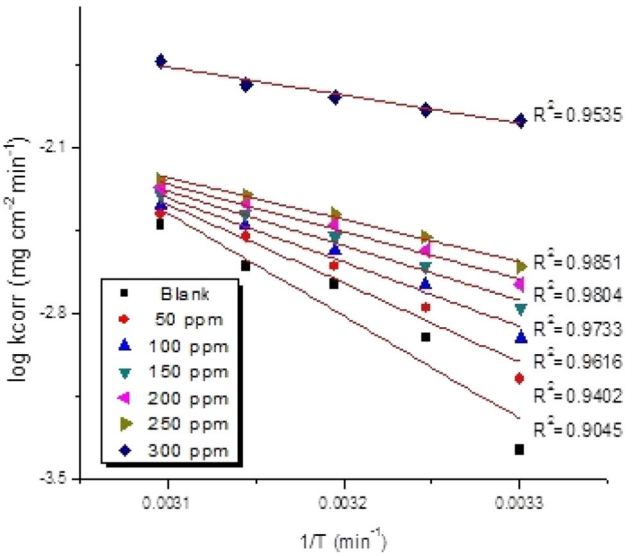

Fig. 3 Arrhenius plots for C-steel corrosion rates (k_{corr}) after 120 min of immersion in polluted NaCl in the absence and presence of various concentrations of AOE

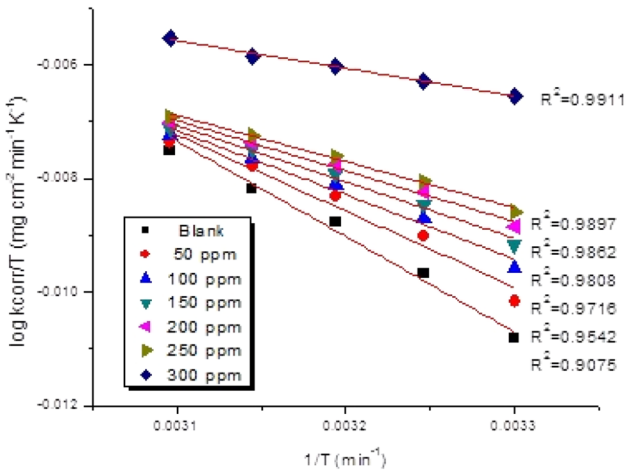

Fig. 4 Transition state for C-steel corrosion rates (k_{corr}/T) in polluted NaCl in the absence and presence of various concentrations of AOE

Table 3 Activation parameters for C-steel corrosion in the absence and presence of various concentrations of AOE in polluted NaCl

[inh] (ppm)	E_a^*(kJ mol^{-1})	ΔH^* (kJ mol^{-1})	$-\Delta S^*$ (J mol^{-1} K^{-1})
Blank	83.2	92.7	197.3
50	63.9	155.6	197.1
100	52.0	170.4	197.1
150	44.2	189.7	197.0
200	38.5	216.2	197.0
250	34.2	256.2	196.8
300	22.8	321.1	196.6

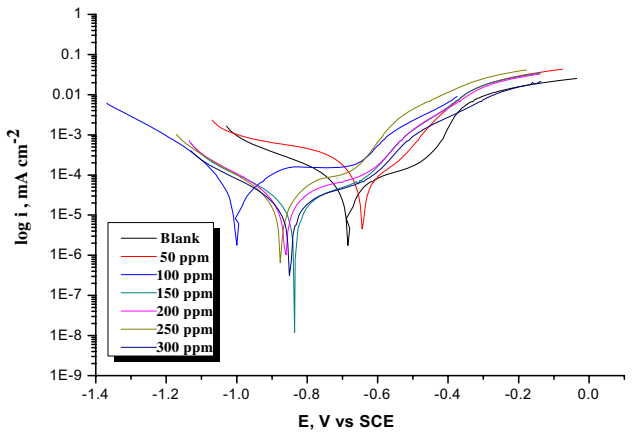

Fig. 5 Potentiodynamic polarization curves for the dissolution of C-steel in polluted NaCl in absence and presence of different concentrations of AOE at 25 °C

are listed in Table 5. The data observed that the corrosion current densities decrease by increasing the concentration obesum extract while the inhibition efficiency (% IE) increases. The causality factors are close to their theoretical values. From EFM measurements, the values of i_{corr} are often obtained directly and freelance of the information about Tafel constants. The % IE is often calculated as in Eq. 4. The intermodulation spectra obtained from EFM in absence and presence of different concentration of AOE are shown in Fig. 6

3.6 EIS Measurements

The EIS of C-steel in the various concentration of AOE is shown in Fig. 7a, b where Fig. 7a is Nyquist plot and Fig. 7b is Bode plot. The curves show that there are gradual increases in the shape of each semicircle of the Nyquist curves by increasing the concentration of the extract. The obtained EIS parameters (R_{ct}), the double layer capacitance, (C_{dl}) and the (% IE) are listed in Table 6. These knowledge shows that there is a rise in (R_{ct}) whereas the (C_{dl}) declined. Due to electrode surface homogeneities and the roughness, the curves obtained from the Nyquist plots are not perfect semicircle.

3.7 SEM Examination

Figure 8 demonstrates the micrograph given for C-steel sheets in the absence and utilizing 300 ppm of AOE after dipping for just 1 day

3.8 Atomic Force Microscope (AFM) Analysis

AFM may be a new technique to review the influence of extract on the generation and also the progress of corrosion at the metal surface. The main advantage of this methodology is that the roughness of the surface may be determined. Figure 9a demonstrates AFM picture of CS example before submersion in contaminated NaCl in 3D. Figure 9b is a picture for CS example after inundation in dirtied NaCl without removes in 3D. Figure 9c alludes to CS example after 24 h in drenching of contaminated NaCl + 300 ppm of AOE in 3D. As shown in Table 7, the lower roughness values in presence of extract, indicate the adsorption of extract molecules on CS surface. In this way, it restrains the corrosion of CS in dirtied NaCl, recommended that the concentrate goes about as great consumption inhibitor. The lower estimation of harshness within the sight of *A. obesum* proposed that *A. obesum* ensures the CS surface in contaminated NaCl.

Table 4 Effect of concentration of AOE on the electrochemical parameters calculated using potentiodynamic polarization technique for the corrosion of C-steel in polluted NaCl at 25 °C

Concentration (ppm)	$-E_{corr}$ (mV) vs SCE	i_{corr} (μA cm^{-2})	β_a (mV dec^{-1})	β_c (mV dec^{-1})	CR (mpy)	θ	% IE
Blank	867.0	301.0	866	260	137.4	–	–
50	642.5	114.0	153	178	52.24	0.621	62.1
100	835.0	32.3	190	390	14.76	0.892	89.2
150	882.0	29.7	160	208	13.58	0.901	90.1
200	1.000	25.4	289	160	11.63	0.916	91.6
250	875.0	25	274	84	11.5	0.917	91.7
300	849.0	9.77	290	121	4.46	0.968	96.8

Table 5 Electrochemical kinetic parameters obtained by EFM technique for dissolution of C-steel in polluted NaCl in absence and presence of different concentrations of AOE at 25 °C

Concentration (ppm)	i_{corr} (μA cm^{-2})	β_a (mV dec^{-1})	$-\beta_c$ (mV dec^{-1})	CF-2	CF-3	CR (mpy)	θ	% IE
Blank	256.90	127	188	1.265	2.471	121.5	–	–
50	87.90	129	139	1.772	2.360	40.18	0.657	65.7
100	70.36	97	181	1.610	1.680	32.15	0.726	72.6
150	65.75	97	196	1.668	1.998	30.04	0.744	74.4
200	57.44	96	153	2.022	2.649	26.25	0.774	77.4
250	43.47	71	74	2.857	4.913	19.86	0.830	83.0
300	33.88	76	107	1.680	1.888	15.48	0.868	86.8

3.9 Fourier Transform Infrared Spectroscopy (FT-IR) Analysis

The FT-IR range is a ground-breaking instrument which used to research the compound utilitarian gatherings and their collaborations with the metal surface. Since natural mixes, for example, drugs are consumed on the metal surface which enhances opposition against consumption, and FT-IR can be utilized to break down the surface changes to demonstrate the idea of the synthetic segments which adsorbed on the surface [29].

Figure 10 shows that the intra-molecular hydrogen bonding of O–H stretching has shifted from 3477 to 3332 cm^{-1}, the –C=C stretching frequency appears at 1635 cm^{-1} (multiple bands), the sharp one at 1019 cm^{-1} referring to –CO stretching, the frequency at 2870, 2948 cm^{-1} is due to –CH stretching, the frequency at 1245 cm^{-1} referred to –CN stretching frequency. These movements in IR spectra allude to the mix between AOE and C-steel happened by means of existing utilitarian gatherings in it. Other practical gatherings have been truant, prescribing that by means of the inhibitor adsorption on the CS surface may have happened through these truant groups [30].

3.10 Antimicrobial Sensitive Test

The results showed that methanolic extract has effective on the antibacterial activity against Gram-positive bacteria

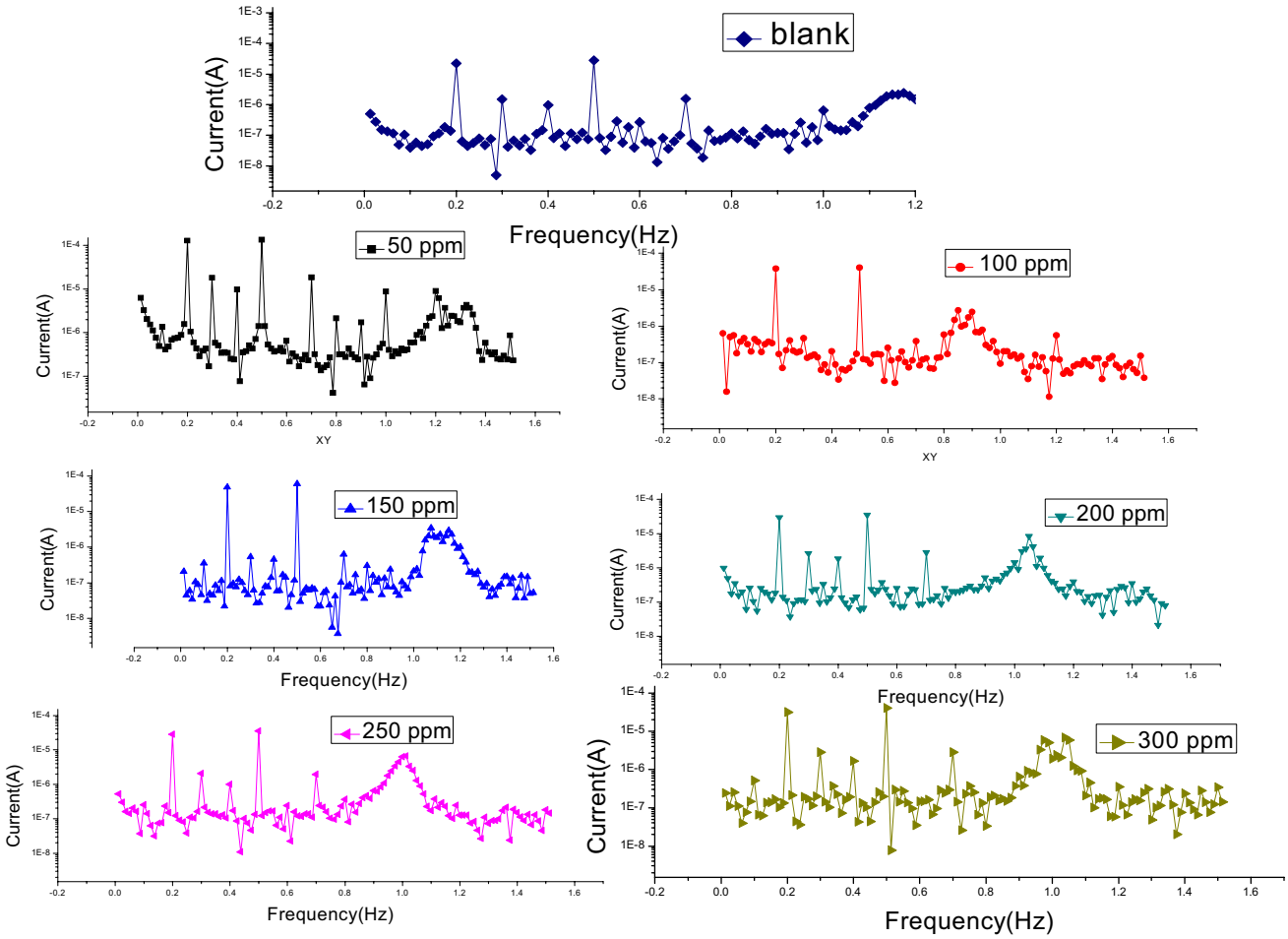

Fig. 6 Intermodulation spectrums for dissolution of C-steel in polluted NaCl in absence and presence of different concentrations of AOE at 25 °C

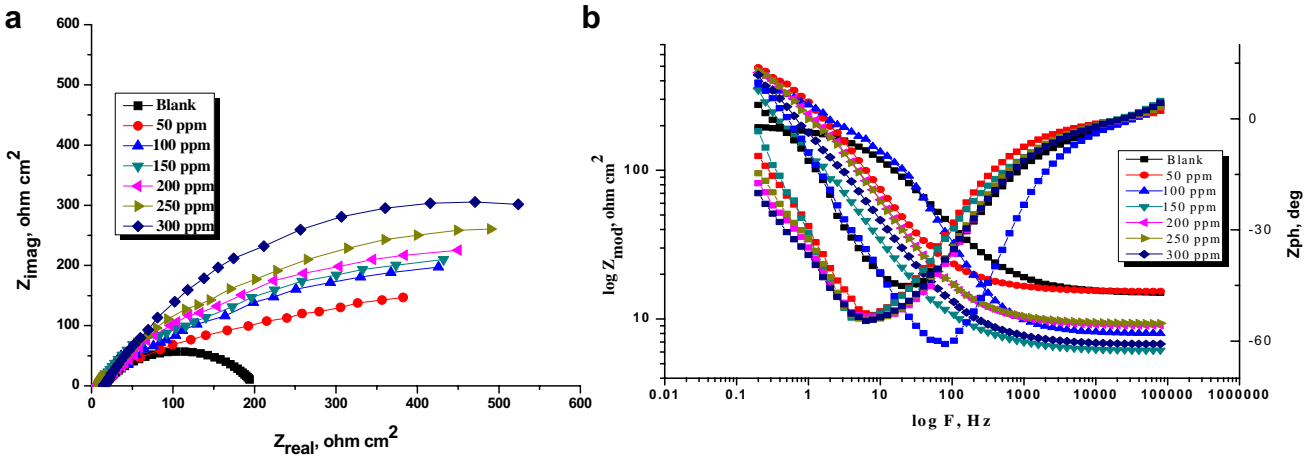

Fig. 7 **a** Nyquist plots recorded for dissolution of C-steel in polluted NaCl in the absence and presence of different concentrations of AOE at 25 °C. **b** Bode plots recorded for dissolution of C-steel in polluted NaCl in absence and presence of different concentrations of AOE at 25 °C

Table 6 Electrochemical kinetic parameters obtained from EIS technique for dissolution of C-steel in polluted NaCl in absence and presence of different concentrations of AOE at 25 °C

Concentration (ppm)	R_{ct} (Ω cm^2)	C_{dl} (μF cm^{-2})	θ	% IE
Blank	110.5	3.704	–	–
50	304.2	0.0831	0.637	63.7
100	661	0.806	0.833	83.3
150	724.4	0.876	0.847	84.7
200	727.8	1.403	0.848	84.8
250	981.7	0.782	0.887	88.7
300	1664	4.535	0.933	93.3

and ineffective against Gram-negative bacteria as reported before [31]. The study suggests that leaves of *A. obesum* (Desert rose) plant can be used as an antimicrobial agent and expected that leaves of *A. obesum* may be used as therapeutic agents for various diseases.

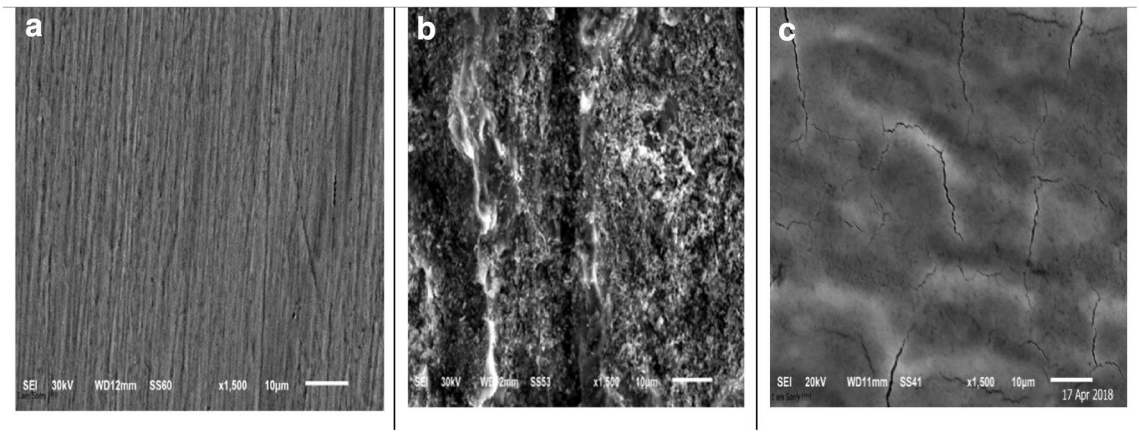

Fig. 8 **a** SEM of metal, **b** SEM of metal + polluted NaCl, metal and **c** SEM of metal + polluted NaCl + 300 ppm of AOE

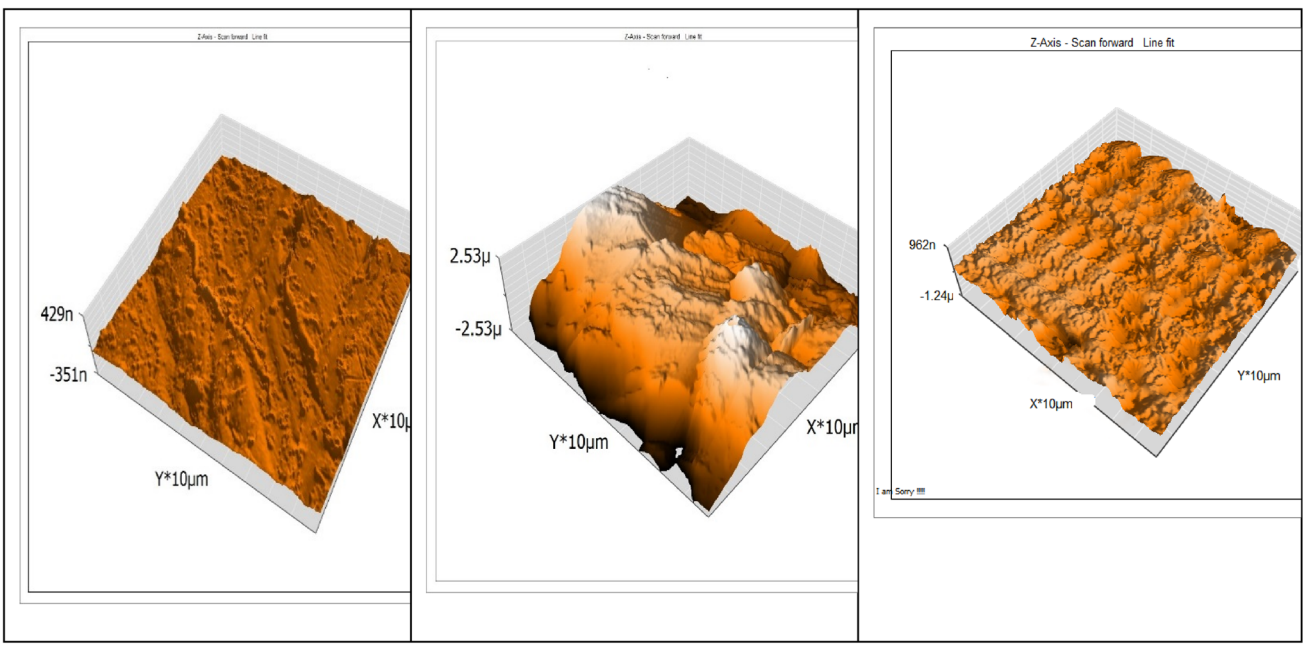

Fig. 9 AFM images of CS surface **a** before immersion in polluted NaCl, **b** after 24 h immersion in polluted NaCl and **c** after 24 h immersion in polluted NaCl + 300 ppm of AOE at 25 °C

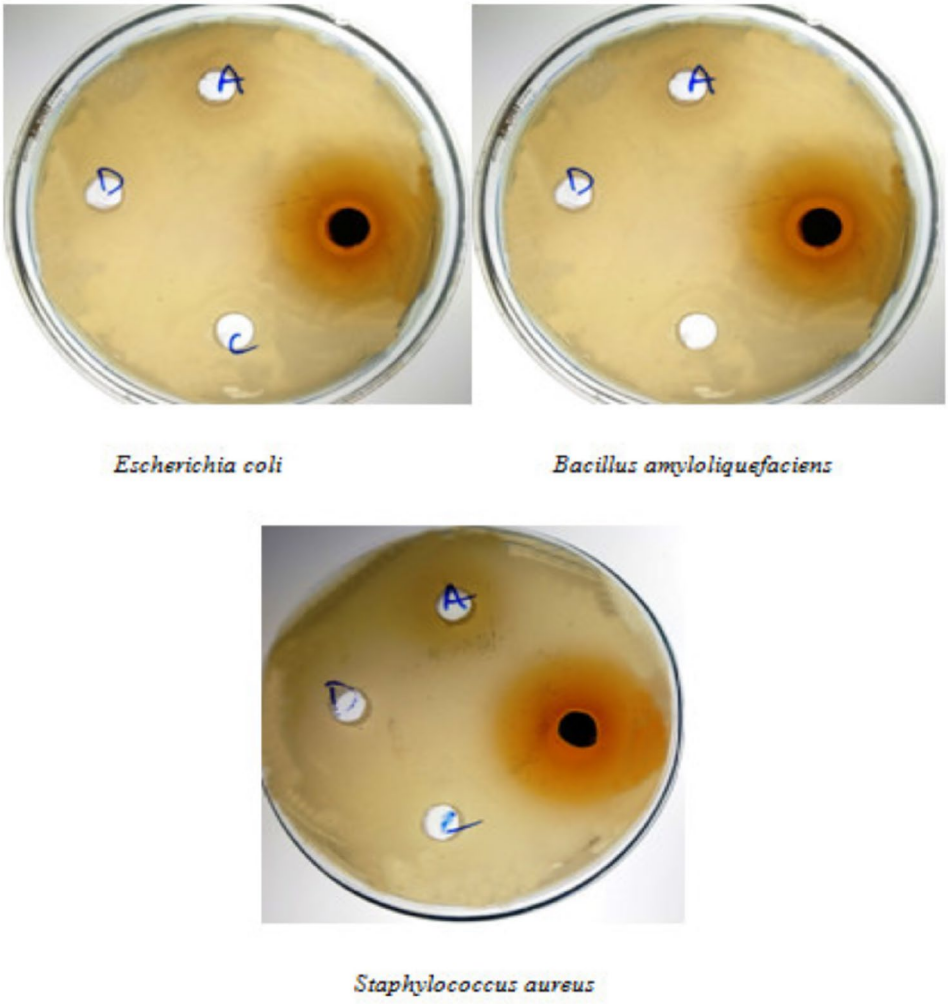

Table 7 AFM parameters for CS (a) pure coin (b) with for 24 h (c) with corrosive medium containing 300 ppm AOE for 24 h

Parameters	a	b	c
The roughness average (S_a)	17.46	993.76	172.7
The mean value (S_m)	− 9.4478	11.064	− 15.88
The root mean square (S_q)	22.976	1234.9	271.0
The valley depth (S_v)	− 108.22	− 5.068	− 770.2
The peak height (S_p)	151.72	2710.1	806.7
The peak-valley height (S_y)	259.93	7.7781	1576.9

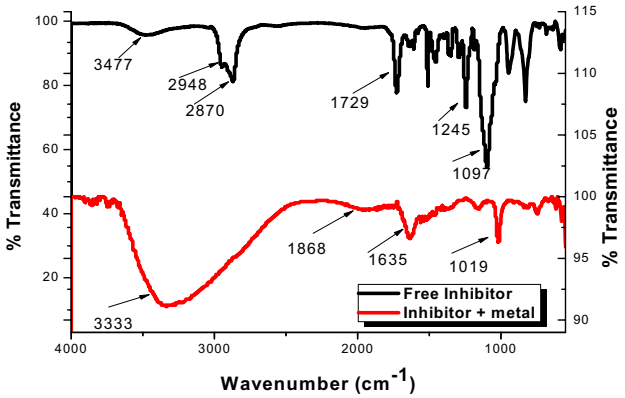

Fig. 10 FT-IR spectroscopy of (a) AOE and (b) the film formed on the CS surface after inundation in polluted NaCl + 300 ppm of AOE for 24 h at 25 °C

Antibacterial activity against *Escherichia coli*, *Bacillus amyloliquefaciens* and *Staphylococcus aureus*. (A) Aqueous extract, (B) methanolic extract and (C and D) control.

3.11 Mechanism of Corrosion Inhibition

The adsorption might be explained through two fundamental processes: physisorption and chemisorption. For the most part, physisorption needs the presence of both charged species in extract and metal surface which electrically charged. The metal surface charge of the electric field exhibited in the metal/prearrangement interface. In opposition, a chemisorption process may incorporate charge exchange or charge sharing from the inhibitor particles to the metal surface to make a coordination bond. This has been accomplished on account of a positive as a negative charge on the metal surface. The CS has empty or low-energy electron orbitals (Fe^{2+} and Fe^{3+}); on the other hand, components of AOE molecules having some electrons or heteroatom's having lone pairs of electrons, which give to the d-vacant orbitals forming chemical bonds, this is responsible for the chemisorption process [32]. Ordinarily, there have been two categories of restraint components that have been recommended. One has been the formation of polymeric structures with (Fe^{3+}) depending on the related conditions [33]; the other one has been the adsorption of AOE on the C-steel surface.

4 Conclusions

The AOE demonstrates the consumption hindrance for CS in polluted NaCl arrangement, where IE inhibition moved forward by ascent of compound fixation. The IE is diminishing with ascent of temperature coming about because of the destruction of the adsorbed AOE atoms exhibits on the CS surface. The nearness of AOE at first glance takes after Temkin condition. Tafel bends demonstrated that AOE is blended kind inhibitors. C_{dl} is decreased by rising the AOE doses, while R_{ct} increases. The adsorbed inactive layer on the C-steel surface was demonstrated by AFM, SEM, and FT-IR examinations.

References

1. Quraishi MA, Singh A, Kumar Singh V, Kumar Yadav D, Kumar Singh A (2010) Green approach to corrosion inhibition of mild steel in hydrochloric acid and sulphuric acid solutions by the extract of *Murraya koenigii* leaves. Mater Chem Phys 122(1):114–122
2. Behpour M, Ghoreishi SM, Khayatkashani M, Soltani Green N (2012) Approach to corrosion inhibition of mild steel in two acidic solutions by the extract of *Punica granatum* peel and main constituents. Mater Chem Phys 131(2):621–633
3. Abiola OK, James AO (2010) The effects of *Aloe vera* extract on corrosion and kinetics of corrosion process of zinc in HCl solution. Corros Sci 52(2):661–664
4. Ebenso EE, Ibok UJ, Ekpe UJ (2018) Methanol extract of *Rumex vesicarius* L. as ecofriendly corrosion inhibitor for carbon steel in sulfuric acid solution. Chem Sci Trans 7(1):101–111
5. Torres V, Amado R, de Sa C, Fernandez TL, da Silva RC (2011) Inhibitory action of aqueous coffee ground extracts on the corrosion of carbon steel in HCl solution. Corros Sci 53(7):2385–2392
6. Majeed M, Sultan A, Al-Sahlanee H (2013) Effect of *Lavandula stoechas* oil on welded material corrosion in 5.5 M H_3PO_4 solution. J Chem Pharm Res 5(12):1297–1306
7. Odewunmi N, Umoren S, Gasem Z (2015) Utilization of watermelon rind extract as a green corrosion inhibitor for mild steel in acidic media. J Ind Eng Chem 21:239–247
8. Lebrini M, Robert F, Lecante A, Roos C (2011) Corrosion inhibition of C_{38} steel in 1 M hydrochloric acid medium by alkaloids extract from *Oxandra asbeckii* plant. Corros Sci 53(2):687–695
9. Roy P, Karfa P, Adhikari U, Sukul D (2014) Corrosion inhibition of mild steel in acidic medium by polyacrylamide grafted guar gum with various grafting percentage: effect of intramolecular synergism. Corros Sci 88:246–253
10. Li L, Zhang X, Lei J, He J, Zhang S et al (2012) Adsorption and corrosion inhibition of *Osmanthus fragran* leaves extract on carbon steel. Corros Sci 63:82–90
11. Zarrok H, Zarrouk A, Salghi R, Assouag M, Hammouti B (2013) Inhibitive properties and thermodynamic characterization of quinoxaline derivative on carbon steel corrosion in acidic medium. Pharm Lett 5:43–53
12. Fouda AS, Abousalem AS, El-Ewady GY (2017) Mitigation of corrosion of carbon steel in acidic solutions using an aqueous extract of *Titia cordata* as green corrosion inhibitor. Int J Ind Chem 8(1):61–73
13. Harbone NV (1994) Phytochemical methods: a guide to modern techniques of plant analysis, 2nd edn. Chapman and Hall, London, p 425
14. Trease GE, Evans WC (1989) Pharmacognosy, 13th edn. ELBS/Bailliere Tindall, London, pp 345–346, 535–536, 772–773
15. Ameer MA, Fekry AM (2015) Corrosion inhibition by naturally occurring *Hibiscus sabdariffa* plant extract on mild steel alloy in HCl solution. Turk J Chem 39:1078–1088
16. Fouda AS, El-Khteeb AY, Fakih M (2013) Methanolic extract of curcumin as green corrosion inhibitor for steel in NaCl polluted solutions. Indian J Sci Res 4(2):219–227
17. Fouda AS, Abd El-Maksoud SA, Fayed HM (2017) *Delonix regia* leaf extract as environmentally friendly and safe corrosion inhibitor for carbon steel in aqueous solutions. J Electrochem Plat Technol. https://doi.org/10.12850/ISSN2196-0267.JEPT5704
18. Ma H, Chen S, Niu L, Zhao S, Li S, Li D (2002) Inhibition of copper corrosion by several Schiff bases in aerated halide solutions. J Appl Electrochem 32(1):65–72
19. Bosch RW, Hubrecht J, Bogaerts WF, Syrett BC (2001) Electrochemical frequency modulation: a new electrochemical technique for online corrosion monitoring. Corrosion 57:60–70
20. Abdel-Rehim SS, Khaled KF, Abd-Elshafi NS (2006) Electrochemical frequency modulation as a new technique for monitoring corrosion inhibition of iron in acid media by new thiourea derivative. Electrochim Acta 51:3269–3277
21. Fouda AS, Al-Sarawy A, El-Katori E (2010) Thiazole derivatives as corrosion inhibitors for C-steel in sulphuric acid solution. Eur J Chem 1(4):312–318
22. Chakravarthy MP, Mohana KN, Kumar CP (2014) Corrosion inhibition effect and adsorption behavior of nicotinamide derivatives on mild steel in hydrochloric acid solution. Int J Ind Chem 5(2):5–19

23. Saleh M, Atia AA (2006) Effects of structure of the ionic head of cationic surfactant on its inhibition of acid corrosion of mild steel. J Appl Electrochem 36(8):899–905. https://doi.org/10.1007/s10800-006-9147-6
24. Bockris JO, Swinkels DAJ (1964) Adsorption of *n*-decylamine on solid metal electrodes. J Electrochem Soc 111(6):736–748. https://doi.org/10.1149/1.2426222
25. Putilova IN, Balezin SA, Barannik UP (1960) Metallic corrosion inhibitor. Pergamon Press, New York, pp 31–37
26. Khamis E (1990) The effect of temperature on the acidic dissolution of steel in the presence of inhibitors. Corrosion (NACE) 46:476–484
27. Popova A, Sokolova E, Raicheva S, Christov M (2003) Temperature effect on mild steel corrosion in acid media in the presence of benzimidazole derivatives. Corros Sci 45:33–58. https://doi.org/10.1016/S0010-938X(02)00072-0
28. Sherif EM, Park SM (2006) Inhibition of copper corrosion in acidic pickling solutions. Electrochim Acta 51(22):4665–4673. https://doi.org/10.1016/j.electacta.2006.01.007
29. Chen W, Hong S, Li HB, Luo HQ, Li M, Li NB (2012) Protection of copper corrosion in 0.5 M NaCl solution by modification of 5-mercapto-3-phenyl-1,3,4-thiadiazole-2-thione potassium self-assembled monolayer. Corros Sci 61:53–62
30. Wang B, Du Zhang M, Gao J (2011) Electrochemical and surface analysis studies on corrosion inhibition of Q235 steel by imidazoline derivative against CO_2 corrosion. Corros Sci 53:353–361
31. Yash S, Anshita N, Susmita S (2015) Antimicrobial activity and phytochemical screening of *Adenium obesum* leaf. Int J Pharm Bio Sci 6(3):85–92
32. Ehsani A, Mahjani MG, Hosseini M, Safari R, Moshrefi R, Shiri HM (2017) Evaluation of *Thymus vulgaris* plant extract as an eco-friendly corrosion inhibitor for stainless steel 304 in acidic solution by means of electrochemical impedance spectroscopy, electrochemical noise analysis and density functional theory. J Colloid Interface Sci 490:444–451
33. Saliyan R, Adhikari AV (2008) Inhibition of corrosion of mild steel in acid media by N′-benzylidene-3-(quinolin-4-ylthio) propanohydrazide. Bull Mater Sci 31:699–711